

# Enhanced thermoelectric properties of samarium boride

Alif Sussardi<sup>a,b</sup>, Takaho Tanaka<sup>a</sup>, A.Ullah Khan<sup>a</sup>, Louis Schlapbach<sup>a</sup>, Takao Mori<sup>a,b,\*</sup>

<sup>a</sup> International Center for Materials Nanoarchitectonics (WPI-MANA), National Institute for Materials Science (NIMS), Namiki 1-1, Tsukuba 305-0044, Japan

<sup>b</sup> Graduate School of Pure and Applied Sciences, University of Tsukuba, 1-1-1 Tennoudai, Tsukuba 305-8671, Japan

Received 15 June 2015; revised 6 July 2015; accepted 14 July 2015

Available online 22 July 2015

## Abstract

SmB<sub>62</sub> single crystals were successfully grown by the floating zone (FZ) method. The high-temperature thermoelectric properties were investigated, together with magnetic properties and specific heat at low-temperature. The electrical resistivity,  $\rho$ , shows variable-range-hopping (VRH) behavior with significantly lower values than other rare-earth RB<sub>62</sub> (RB<sub>66</sub>) compounds. An effective magnetic moment,  $\mu_{\text{eff}}$ , of 0.42  $\mu_B$ /Sm was estimated, which if straightforwardly taken indicates a mixed valency for SmB<sub>62</sub> with Sm<sup>2+</sup>:Sm<sup>3+</sup> = 1:1, which is the first ever indicated for RB<sub>66</sub>-type compounds. Localization length of the VRH at the Fermi level,  $\xi$ , was estimated to be 3.33 Å indicating that carriers in SmB<sub>62</sub> are much less localized than in YB<sub>66</sub> which has 0.56 Å. The thermoelectric behavior of SmB<sub>62</sub> is striking, with  $\rho$  reduced by two orders of magnitude while maintaining large Seebeck coefficients, and as a result the power factor is ~30 times higher than other rare-earth phases. Overall the figure of merit  $ZT$  amounts to ~0.13 at 1050 K, with an extrapolated value of ~0.4 at 1500 K, an expected working temperature for topping cycles in thermal power plants; that gives a ~40 times enhancement for Sm. Since there are few thermoelectric materials applicable for very-high temperature applications, this discovery gives new interest in the samarium higher borides.

© 2015 The Chinese Ceramic Society. Production and hosting by Elsevier B.V. This is an open access article under the CC BY-NC-ND license (<http://creativecommons.org/licenses/by-nc-nd/4.0/>).

**Keywords:** Thermoelectric; Boride; Samarium boride; Mixed valency; High temperature

## 1. Introduction

Thermoelectric materials are being actively investigated throughout the world now, due to the potential large societal benefits through the direct conversion of waste heat to electricity. One need exists to develop high temperature thermoelectric materials which can utilize the high temperature waste heat in thermal power plants, steelworks, factories, and incinerators, etc. and also the conversion of concentrated solar power CSP [1,2]. The performance of thermoelectric materials can be evaluated by the figure of merit  $ZT = S^2T/\rho\kappa$ , where  $S$ ,  $\rho$ ,  $\kappa$  and  $T$  are the Seebeck coefficient, electrical resistivity, thermal conductivity and temperature, respectively.

Boron cluster compounds are attractive candidates as high temperature thermoelectric materials because of their material stability and generally large Seebeck coefficients [3–5]. Furthermore, they have been found to typically possess intrinsic low thermal conductivity [6–8], which is a built-in advantage for thermoelectrics. This property is quite interesting since the boron cluster compounds are strongly covalently bonded solids with high sound velocities. Several mechanisms, such as symmetry mismatch effect or degrees of freedom of boron dumbbells in the B<sub>80</sub> cluster, in addition to the well-known crystal complexity first demonstrated by Slack [8], have been proposed to be the origin of this intrinsic low thermal conductivity [5,9,10]. Many of the boron cluster compounds follow the variable range hopping (VRH) transport mechanism [11] which is advantageous at high temperatures, since the electrical conductivity and Seebeck coefficient have a positive temperature coefficient [3,4]. Another attractive feature of such boron cluster compounds in general is that the network structures and physical properties have been found to

\* Corresponding author. International Center for Materials Nanoarchitectonics (WPI-MANA), National Institute for Materials Science (NIMS), Namiki 1-1, Tsukuba 305-0044, Japan.

E-mail address: [MORI.Takao@nims.go.jp](mailto:MORI.Takao@nims.go.jp) (T. Mori).

Peer review under responsibility of The Chinese Ceramic Society.

be controllable to some degree through incorporation of metal atoms in the voids of clusters, and also by the addition of third elements like C, N, Si which can act as bridging sites of the cluster framework [12].

Up to now, there has been active investigation into the thermoelectric properties of boron cluster compounds such as boron carbide [2,13–15], rare earth borocarbonitrides  $RB_{15.5}CN$ ,  $RB_{22}C_2N$ , and  $RB_{28.5}C_4$  ( $R$  = rare earth) [16–19], doped  $\beta$ -boron [20–22],  $B_6S_{1-x}$  [23],  $RB_{66}$  [24,25],  $RB_{44}Si_2$  [3,8,26,27],  $MgAlB_{14}$  [28,29],  $Y_xAl_yB_{14}$  [30–32], and a recent re-examination of the prospects of  $B_6O$  by Slack [33].

$RB_{66}$  is an interesting boride [12], with a complex structure with more than 1600 atoms in the unit cell, and it was discovered to be a crystalline material with glass-like thermal conductivity [5,6], which can be considered as a precursor to the famous phonon glass electron crystal (PGEC) concept. A view of the crystal structure is given in Fig. 1, together with a simplified view. The crystal structure can be represented by three structural units; the  $(B_{12})_{13}$  supericosahedra,  $B_{80}$  cluster, and the rare earth atoms. As a representative expression of the compound,  $RB_{66}$  is typically used, but the congruent composition has been reported to be  $RB_{62}$ , for example, and in some

cases the composition is also used to express the compound (like in this paper).

Among rare-earth series of compounds, phases with Yb and Sm have been discovered to sometimes exhibit anomalous properties for different reasons, related e.g. to mixed valency [34]. Mixed valency has previously been reported in the case of  $SmB_6$  [35–37]. Recently,  $SmB_6$  has attracted increasing interest as a topological insulator [38–45]. Topological insulators have been reported to have enhanced thermoelectric properties [46].

With these developments in mind, we revisited the PGEC  $RB_{66}$  compound and investigated the samarium phase in detail by growing high quality single crystals of  $SmB_{62}$ .  $RB_{66}$  (congruent composition of  $RB_{62}$ ) had previously been reported to be a poor thermoelectric material [24,25] but we discovered that  $SmB_{62}$  has a  $\sim 40$  times higher  $ZT$  than its yttrium and erbium counterparts. At 1050 K it amounts to 0.13, or extrapolated to 1500 K (an expected working temperature for topping cycles in thermal power plants) a value of  $\sim 0.4$ , which is a promising start as a new high temperature material. This discovery of a dramatic increase in performance in a well-known boride by investigating the samarium phase, is exciting and shows the still untapped potential of these materials.

## 2. Experimental

$SmB_{62}$  crystals were synthesized by the Floating Zone (FZ) method with focused light from four Xenon lamps. The feed and seed rod for the crystal growth were synthesized by the borothermal reduction method [12], starting from samarium oxide and boron powder.

The borothermal reduction method was carried out by mixing  $Sm_2O_3$  (99.95% Wako) and Boron (99.9% SB Boron) with ratios of B: $Sm_2O_3$  of 127:1 and 123:1 to make the composition Sm:B to be 1:62 and 1:60, respectively. We used a composition of  $SmB_{62}$ , since this has been shown to be the congruent composition for  $YB_{66}$ , and we therefore, tried to grow a slightly samarium-rich crystal also. The constituents were mixed in agate mortars for 20 min in ethanol to ensure homogeneity. After drying the mixture overnight under a halogen lamp, it was compacted with a Cold Isostatic Press (CIP) apparatus at 2500 kg/cm<sup>2</sup> to form solid rods. Then the solid rods were heated in an induction furnace for 8 h at  $\sim 1700$  °C under vacuum. The temperature was controlled manually with a pyrometer.

The rods were then crushed with a mortar and compacted by CIP and heated again by induction furnace. The process was repeated 3 times to be certain to reduce  $Sm_2O_3$  completely and form the samarium boron solid rod. BO gas was observed to emanate during heating, with the most intense gas evaporation observed during the first heating sequence, but reduced considerably for following sequences. At the end of the borothermal reduction process, the rods were dense and ready to be used as feed and seed rod for FZ crystal growth. A part of the rod was crushed and characterized by powder X-ray diffraction (XRD) using a Rigaku Ultima III X-ray

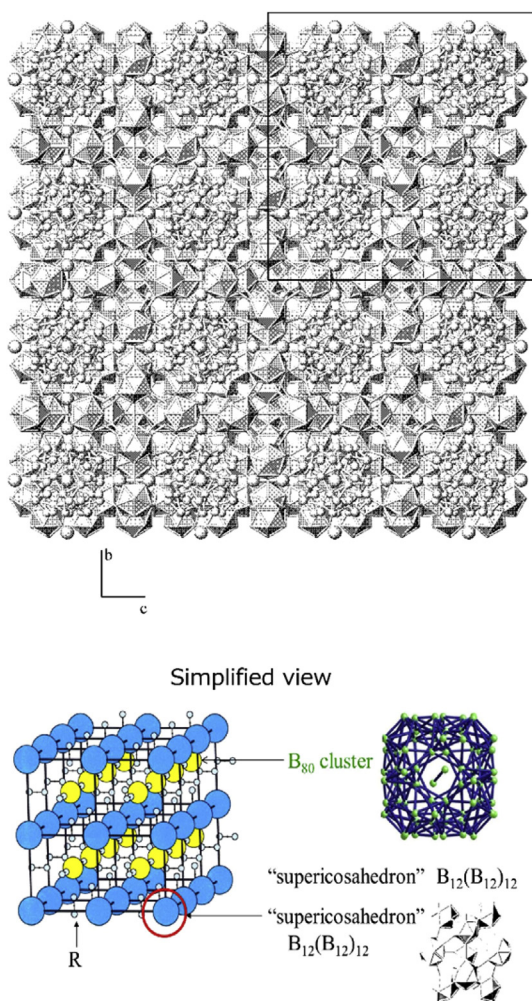


Fig. 1. Crystal structure of  $RB_{62}$  ( $RB_{66}$ ).

Diffractometer just as a check of the phase. Pieces of the grown crystals were finally crushed for XRD characterization. Rietveld refinement was carried out using the FullProf Suite Program (2.05). The rod was then divided in 2 parts, the small part utilized as seed rod and the longer part utilized as feed rod. The FZ crystal growth was performed by focusing four Xenon lamps to create the molten zone in the rod, and then the feed and seed rod were pulled down to grow the crystal. The optimum growth rate for  $\text{SmB}_{62}$  was found to be 8 mm/h. The seed rod was rotated clockwise at 10 rpm and the feed rod was rotated counter-clockwise at 15 rpm. The crystals were grown in a way to have approximately 10 mm in diameter.

Thermal conductivity measurements were carried out with the laser flash method using an ULVAC TC7000, to determine the thermal diffusivity and relative specific heat, from which thermal conductivity can be determined. The absolute specific heat value at low temperature and room temperature was measured by a PPMS (Quantum Design). The specific heat at high temperature was measured by Differential Scanning Calorimetry Rigaku Thermo Plus Evo 2 up to 773 K, and from 873 K up to 1073 K was calculated from  $C_p$  and  $1/\Delta T$  (inverse of the temperature rise due to the laser pulse). The magnetic susceptibility was measured with a MPMS (Quantum Design). The electrical resistivity and Seebeck coefficient measurements were carried out with an ULVAC ZEM-2. Scanning electron microscope (SEM) images of the crystals were taken by a Hitachi FE-SEM S-4800. The images were taken from polished samples after coating with platinum by RF sputtering.

### 3. Results and discussions

A picture of the floating zone (FZ) grown  $\text{SmB}_{60}$  crystal, and samples cut for measurements, are shown in Fig. 2. The disc is for laser flash measurements, and bar for Seebeck and electrical conductivity measurements. The striations on the surface of the cut samples are due to the cutting with the diamond saw. The directions of the measurements are approximately parallel to the long axis of the crystal for the thermal conductivity and perpendicular for the Seebeck and electrical conductivity, but since this compound is isotropic this should not have any significant effect.

The powder x-ray diffraction patterns of  $\text{SmB}_{62}$  and  $\text{SmB}_{60}$  crystals are shown in Fig. 3. The majority phase matches the  $\text{RB}_{66}$ -type crystal structure. There is a small amount of impurity phase  $\text{SmB}_6$  in  $\text{SmB}_{62}$  and  $\text{SmB}_{60}$  crystals (0.25% and



Fig. 2. FZ grown  $\text{SmB}_{60}$  crystal, and cut samples for measurements.

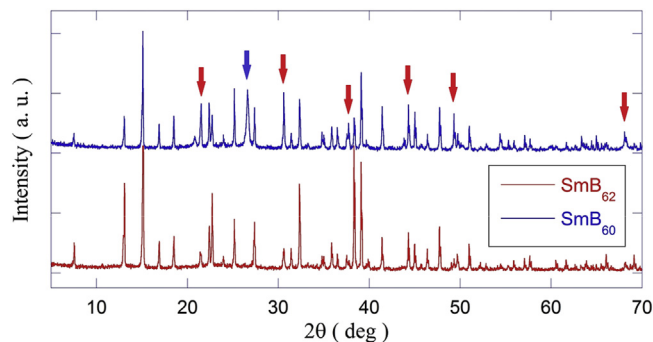


Fig. 3. X-ray diffraction patterns from  $\text{SmB}_{62}$  (bottom) and  $\text{SmB}_{60}$  (top) crystals. For the  $\text{SmB}_{60}$  crystal, red and blue arrows show the  $\text{SmB}_6$  and carbon impurity phases, respectively.

1.8%, respectively), as determined by the Rietveld refinement. We also found a carbon impurity as shown by the blue arrow for the  $\text{SmB}_{60}$  crystal, which might be caused by the heating process inside the induction furnace, where inert boron nitride crucibles are used but with heating elements of graphite outside. For the  $\text{SmB}_{62}$  crystal, we used a specially designed carbon-free heating element [12] and were able to avoid the carbon impurity. These impurities appear not to have a big effect on the thermoelectric properties as seen later. The Rietveld refinement yielded the lattice parameters as 23.493(8) Å and 23.466(1) Å for the  $\text{SmB}_{62}$  and  $\text{SmB}_{60}$  crystals, respectively. The measured densities of  $\text{SmB}_{60}$  and  $\text{SmB}_{62}$  crystals are 2.755 and 2.650 g/cm<sup>3</sup> which correspond to 98.7% and 99% of the theoretical density, respectively. To our knowledge, this is the first report of floating zone crystal growth of  $\text{SmB}_{66}$ -type single crystals. Previous synthesis of  $\text{SmB}_{66}$  has been carried out by sintering or melt methods [47–49].

The chemical composition of  $\text{SmB}_{62}$  was confirmed using Electron Probe Micro-Analysis (EPMA). In the case of the  $\text{SmB}_{60}$  crystal, the composition consists of the  $\text{SmB}_{62}$  phase and a larger content of impurity  $\text{SmB}_6$  phase. Furthermore, from the SEM pictures of Fig. 4(a) and (b), we can see that there are many submicron pores in the  $\text{SmB}_{60}$  crystal. In contrast, for  $\text{SmB}_{62}$ , no sizable pores in the crystal were observed.

To summarize the results of the crystal growth, attempts to obtain a more metal-rich  $\text{SmB}_{62}$  crystal of  $\text{SmB}_{60}$ , results in a larger amount of  $\text{SmB}_6$  impurities, and furthermore, submicron pores were also created in the crystal, despite our careful tuning of the optimum crystal growth conditions. It appears that high quality  $\text{SmB}_{66}$  crystal growth is much more difficult than  $\text{YB}_{66}$ , for example, which has shown a wide homogeneity region and easier crystal growth from  $\text{YB}_{56}$  to  $\text{YB}_{68}$  [50,51].

So far measurements of the Seebeck coefficient of  $\text{SmB}_{66}$  were reported just for 300 K to be 100  $\mu\text{VK}^{-1}$  [49]. Results of our electrical resistivity  $\rho$  and Seebeck coefficient  $S$  measurements of FZ grown  $\text{SmB}_{60}$  and  $\text{SmB}_{62}$  crystals are plotted in Fig. 5. Comparing the data at 300 K with Golikova's results reveals that our crystals show a 5 times larger Seebeck coefficient and a slightly higher resistivity. This may be due to some change in composition (detailed characterization

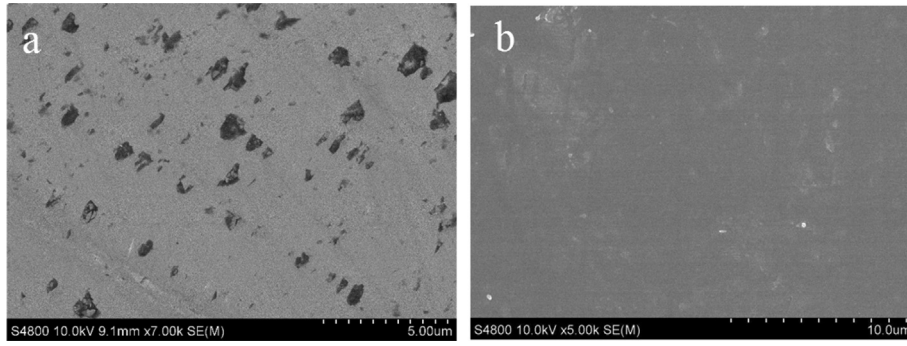


Fig. 4. SEM images of the crystals; (a)  $\text{SmB}_{60}$  with pores and (b)  $\text{SmB}_{62}$ , the higher quality crystal without pores. White spots are due to the polishing powder.

analysis appear not to have been carried out for Golikova's samples), but in any case our FZ grown crystals appear to have much more attractive thermoelectric properties. For the FZ grown crystals,  $\text{SmB}_{60}$  has slightly lower electrical resistivity at low temperatures as compared to  $\text{SmB}_{62}$ , despite having

some pores. This may be due to the existence of graphitic carbon impurities and larger amount of  $\text{SmB}_6$  which are both highly conductive, as observed before in composite effects in other systems with metallic impurity doping [17,52,53]. A large difference in the electrical resistivity between the Sm phase and other rare earth phases of Y [25] and Er [26], with almost 2 orders lower resistivity for  $\text{SmB}_{60}$  and  $\text{SmB}_{62}$  crystals, while the Seebeck coefficients do not show such a large reduction.

The electrical conductivity of the boron icosahedra compounds in general follow the three-dimensional variable range hopping (VRH) by Mott [11]. Mott's variable range hopping is based on the probability for electrical carriers in a specific material to hop (i.e. be transported) by increasing temperature, and where for 3 dimensional systems, the resistivity follows the relationship:

$$\rho = \rho_0 \exp \left[ (T_0/T)^{0.25} \right]. \quad (1)$$

The  $\rho_0$  and  $T_0$  is resistivity pre-factor and characteristic temperature, respectively. As shown by the  $\log \rho$  versus  $T^{-0.25}$  plot in Fig. 6, the electrical resistivity generally follows a straight line indicating the VRH dependence. The determined  $\rho_0$  and  $T_0$  values of the materials from fitting with Eq. (1) are summarized in Table 1

Fig. 7 shows the temperature dependence of the magnetic susceptibility of the  $\text{SmB}_{62}$  crystal. The Curie–Weiss fit,

$$\chi = \frac{C}{T - T_c} \quad (2)$$

gives us an effective magnetic moment of 0.42 Bohr magnetons ( $\mu_B$ ) per Sm atom. This is about half the effective magnetic moment expected for a free trivalent  $\text{Sm}^{3+}$  ion. Previously it has been reported that  $\text{SmB}_6$  is a mixed valence compound with  $\text{Sm}^{2+}$ :  $\text{Sm}^{3+}$  ratio of 3:7 [35]. Straightforwardly interpreting these results yields a mixed valence of samarium in  $\text{SmB}_{62}$  with  $\text{Sm}^{2+}$ :  $\text{Sm}^{3+}$  of 1:1. No mixed valence for any other  $\text{RB}_{66}$  has ever been reported. Considering this valence, it seems to be reasonable that we are getting an enhanced hole conduction for  $\text{SmB}_{62}$  compared to the other  $\text{RB}_{66}$  ( $\text{YB}_{66}$  and  $\text{ErB}_{66}$ ). Although we were not able to obtain good Hall measurements to make direct evaluation of the carrier concentration, which difficulty has been generally

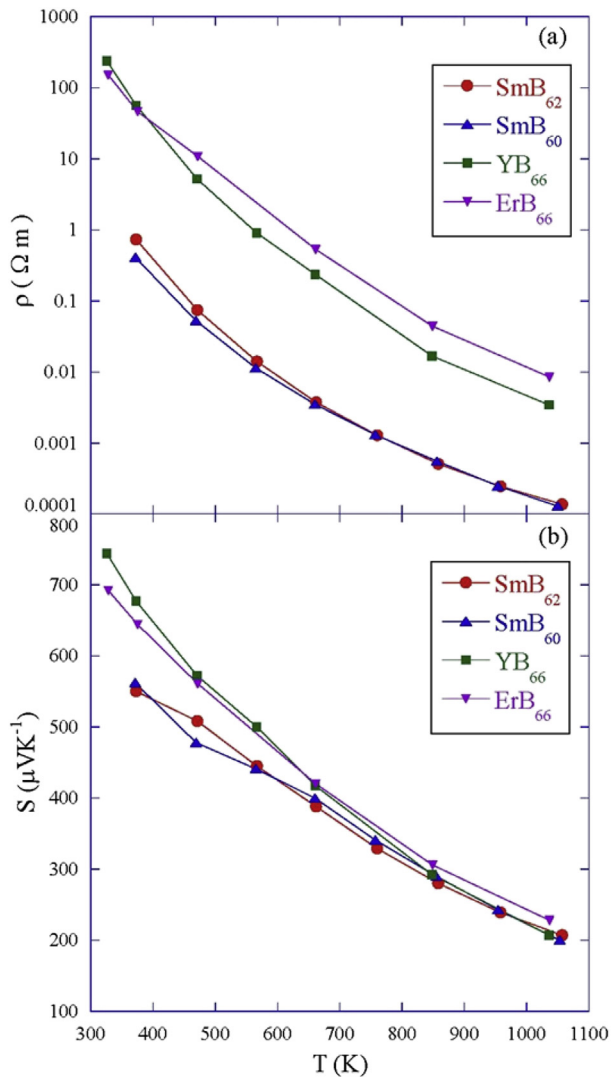


Fig. 5. Temperature dependence of the (a) electrical resistivity  $\rho$ , (b) Seebeck coefficient  $S$ , of  $\text{SmB}_{60}$  and  $\text{SmB}_{62}$  crystals. The values of  $\text{YB}_{66}$  [25] and  $\text{ErB}_{62}$  [26] are plotted from references.

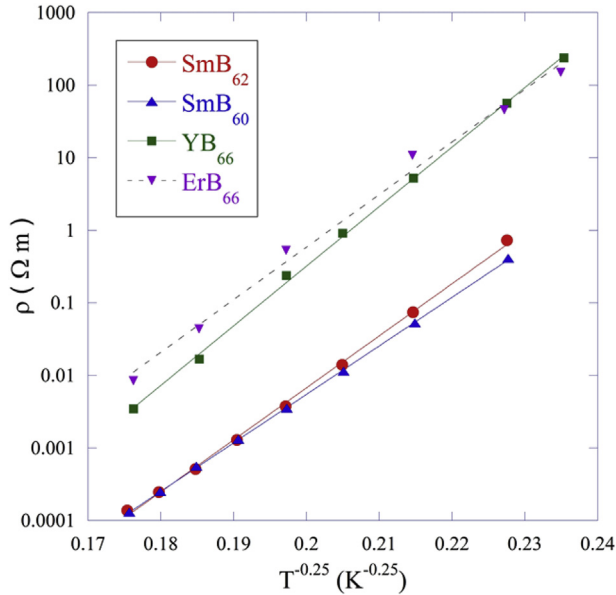


Fig. 6. The logarithmic resistivities of  $\text{SmB}_{60}$  and  $\text{SmB}_{62}$  crystals plotted versus  $T^{-0.25}$ . The values of  $\text{YB}_{66}$  [25] and  $\text{ErB}_{62}$  [26] are plotted from references.

observed for the variable range hopping higher borides, the mixed valency is an obvious indication of increasing number of holes.

Typically for thermoelectric materials, when the carrier concentration is increased, the electrical resistivity decreases, but the absolute value of the Seebeck coefficient also decreases in a trade-off. However, the striking feature is that for  $\text{SmB}_{62}$ , although we observe a huge, almost 2 orders of reduction of the resistivity compared with the yttrium and erbium phases, the Seebeck coefficient values are only slightly decreased, thereby causing  $\sim 30$  times enhancement of the power factor,  $PF = S^2/\rho$  (Fig. 8). Considering this striking result, it would be of interest to see electronic structure calculations on  $\text{SmB}_{62}$ , however, we have not been able to obtain this yet, because of the extremely large unit cell with  $\sim 1600$  atoms in the unit cell. Nevertheless, with increase of calculation power and new methods we hope this will be possible in the near future.

We further analyzed the transport behavior of  $\text{SmB}_{62}$  in comparison with other rare earth phases estimating the localization length  $\xi$  of the variable range hopping (VRH), which has been demonstrated to be a measure of the microscopic disorder for similar systems [9,12].

In VRH systems, the localization length at the Fermi level has the following relationship with the characteristic temperature  $T_0$  determined above

Table 1  
Parameters determined from Mott's variable range hopping (VRH) of the electrical resistivity.

Compound	$\rho_0$ ( $\Omega \text{ m}$ )	$T_0$ (K)
$\text{SmB}_{62}$	$3.08 \times 10^{-17}$	$7.43 \times 10^8$
$\text{SmB}_{60}$	$2.35 \times 10^{-16}$	$5.61 \times 10^8$
$\text{YB}_{66}$ [25]	$1.22 \times 10^{-17}$	$1.28 \times 10^9$
$\text{ErB}_{66}$ [26]	$1.90 \times 10^{-15}$	$7.75 \times 10^8$

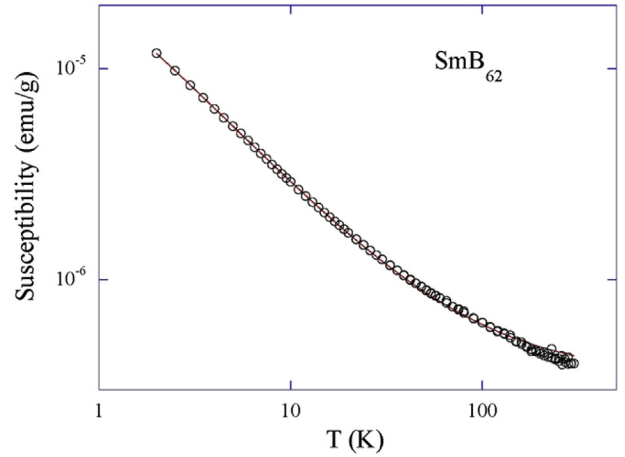


Fig. 7. Temperature dependence of magnetic susceptibility of the  $\text{SmB}_{62}$  crystal. The line indicates the fitting to Eq. (2).

$$k_B T_0 = 1.81 / (D(E_F) \xi^3) \quad (3)$$

where  $k_B$ ,  $D(E_F)$ , and  $\xi$  are Boltzmann constant, density of states at Fermi level energy and localization length. In order to evaluate  $D(E_F)$  we measured the specific heat of  $\text{SmB}_{62}$  at low temperature. The specific heat,  $C$ , can be written as the sum of electron and phonon contributions with an approximation of

$$C = \gamma T + \beta T^3 \quad (4)$$

valid at low temperatures well below the Debye temperature, where  $\gamma$  and  $\beta$  are constants characteristic of the material. The experimental results were plotted as  $C/T$  versus  $T^2$ , shown in Fig. 9. From the linear fitting we obtain  $\gamma$  and  $\beta$  values  $3.0 \times 10^{-2} \text{ mJg}^{-1} \text{K}^{-2}$  and  $2.6 \times 10^{-4} \text{ mJg}^{-1} \text{K}^{-4}$ , respectively. There is a deviation from a straight line at low temperature with  $C/T$  showing an increase probably of magnetic origin [54–56]. The  $\gamma$  value of  $\text{SmB}_{62}$  is equivalent to  $24.7 \text{ mJmol}^{-1} \text{K}^{-2}$  which is relatively large, and could indicate

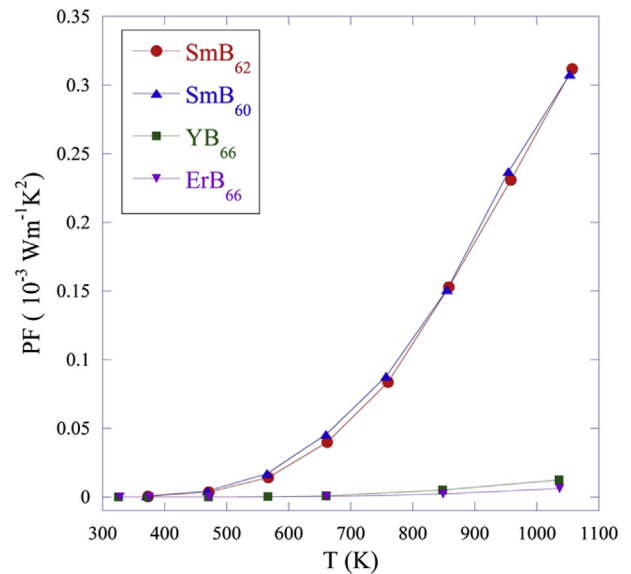


Fig. 8. Temperature dependence of the power factors of  $\text{SmB}_{60}$ ,  $\text{SmB}_{62}$  crystals. The values of  $\text{YB}_{66}$  [25] and  $\text{ErB}_{62}$  [26] are plotted from references.

some strong correlations in the material [34], but in any case, at present, any direct effect of this on high temperature thermoelectric properties is not clear.

The electronic  $\gamma$  coefficient of the specific heat follows the relationship:

$$\gamma = 1/3\pi^2 k_B^2 D(E_F) \quad (5)$$

And we can substitute Eq. (5) to Eq. (3) to obtain the localization length.

$$\xi = \sqrt[3]{\frac{18.1\pi^2 k_B}{3\gamma T_0}} \quad (6)$$

The localization length of SmB<sub>62</sub> obtained from calculation is 3.33 Å, compared to the YB<sub>66</sub> localization length from the literature which is 0.56 Å, indicating that SmB<sub>62</sub> electronic states are significantly less localized as compared to YB<sub>66</sub>.

This reduced localization may be related to the origin of the huge enhancement of the power factor of SmB<sub>62</sub> compared to the other rare earth phases. The origin should be further studied, with a detailed investigation of the mixed valence behavior, of strong correlation effects, and also of potential of topological insulating states as was previous reported for SmB<sub>6</sub>.

As regards the thermal properties, we plot the heat capacity, thermal diffusivity, and thermal conductivity, in Fig. 10(a), (b), and (c), respectively. The thermal conductivity values of  $\kappa$  of SmB<sub>62</sub> and SmB<sub>60</sub> are somewhat lower than YB<sub>66</sub> [6]. This trend can be understood by considering the much larger mass of Sm compared to Y. The SmB<sub>60</sub> crystal has higher thermal conductivity than SmB<sub>62</sub>, which is interesting considering the pores observed in SmB<sub>60</sub>, but which is likely due to the effect of higher content of impurities in SmB<sub>60</sub>, namely SmB<sub>6</sub> and carbon. We also plot the lattice thermal conductivity,  $\kappa_L$ , estimated using a Lorenz number of  $1.5 \times 10^{-8} \text{ W}\Omega\text{K}^{-2}$ . This

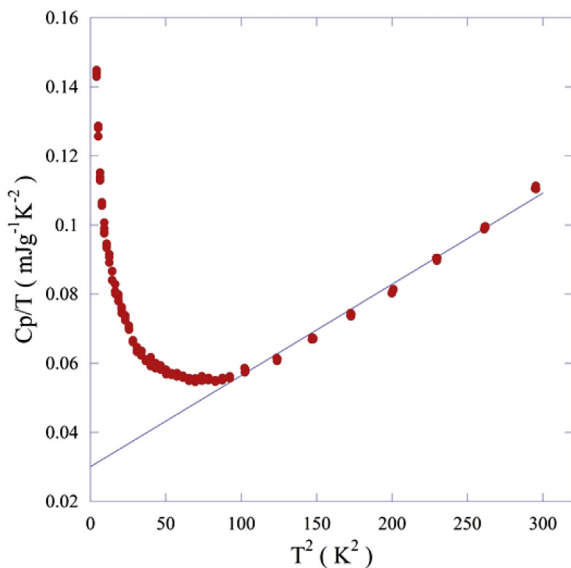


Fig. 9.  $C_p/T$  versus  $T^2$  plot for the SmB<sub>62</sub> crystal. The line shows the linear fitting with the upturn below  $T = 10$  K possibly due to magnetic behavior at lower temperatures.

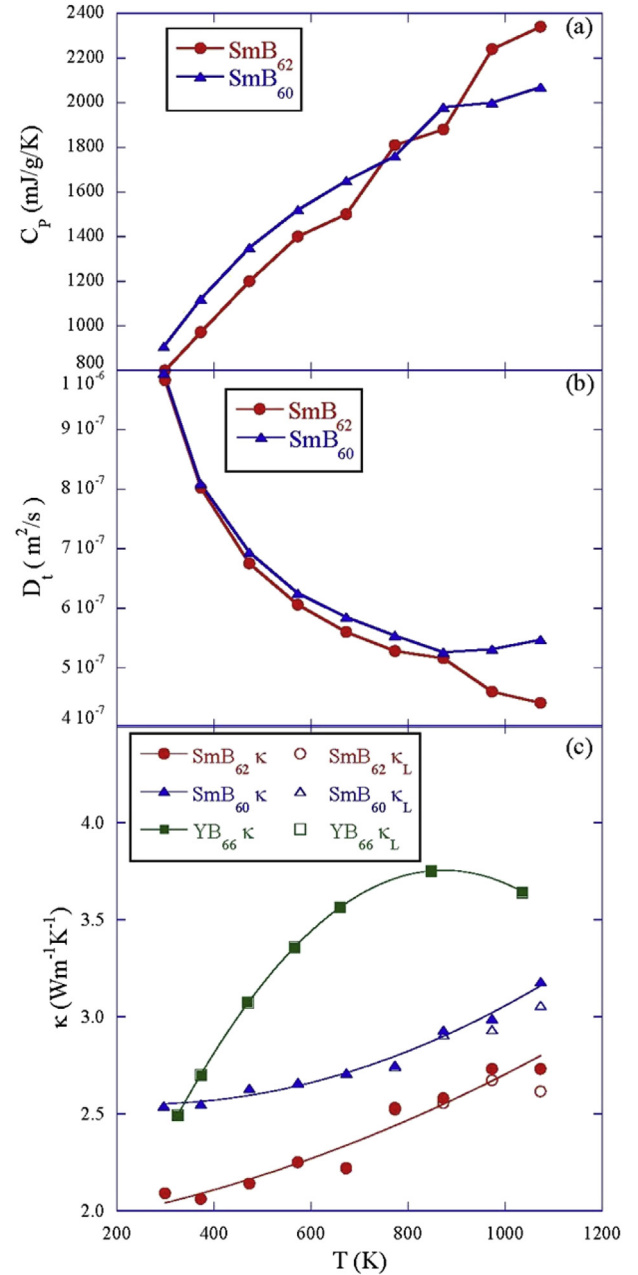


Fig. 10. Temperature dependence of the (a) heat capacity, (b) thermal diffusivity, and (c) thermal conductivity and lattice thermal conductivity of SmB<sub>60</sub> and SmB<sub>62</sub> crystals. The thermal conductivity of YB<sub>66</sub> [6] is also plotted for comparison.

of course will give an upper limit to  $\kappa_L$  but determination of the Lorenz number for this complex variable range hopping system is not trivial. In any case, we can observe that the thermal conductivity is dominated by the lattice thermal conductivity, as has generally been the case for these higher borides with relatively low electrical conductivity.

The estimated figure of merit of SmB<sub>60</sub> is  $\sim 0.13$  at 1050 K, approximately 40 times bigger than YB<sub>66</sub> as shown in comparison in Fig. 11. One of the main interests for very-high temperature thermoelectric materials is their possibility to be utilized in topping cycles in thermal power plants to enhance the total output power [57–59]. A working temperature could

be 1500 K, which by itself is not a problem for  $\text{SmB}_{62}$  as the melting point is around 2850 K [60,61]. With this in mind, we extrapolate the  $ZT$  to 1500 K to yield an extrapolated value of  $\sim 0.4$ . The directly obtained value of 0.13 is not relatively high, but can be expected to be improved since these are the initial results for an unmodified compound. Starting with work by Slack on elemental boron, doping with transition metals has been shown to be a powerful way to enhance the thermoelectric properties of boron cluster compounds [4,15,20,21]. A beneficial hybrid effect was also previously obtained for the  $n$ -type counterpart compound to boron carbide, whereby with a combination of transition metal doping and heat treatment, the Seebeck coefficients of  $\text{YB}_{22}\text{C}_2\text{N}$  could be increased by up to 220% while resistivity was simultaneously very largely reduced by 2 orders [52,53]. Considering that work on samarium higher boride has just started, we think the present results provide a promising starting point for further development as very-high temperature thermoelectric materials.

#### 4. Conclusion

We grew  $\text{SmB}_{60}$  and  $\text{SmB}_{62}$  single crystals by the floating zone (FZ) method and investigated their thermoelectric properties. These Sm phases show striking enhancement of the thermoelectric properties compared to those of other rare earth phases of the  $\text{RB}_{62}$  ( $\text{RB}_{66}$ ) family like  $Y$  and  $Er$ , with slightly lower Seebeck coefficients and very large increase of electrical conductivity by almost 2 orders of magnitude, leading to a power factor enhancement of  $\sim 30$  times.

We interpret the magnetic properties with a mixed valence behavior with the ratio of  $\text{Sm}^{2+}:\text{Sm}^{3+} = 1:1$ . This is the first mixed valence behavior ever reported for the  $\text{RB}_{66}$ -type compounds, and indicates enhanced hole conduction. However, the striking point is that despite the very largely increased electrical conductivity, unlike with the typical tradeoff relationship, the

Seebeck coefficient does not decrease significantly, leading to the strongly enhanced thermoelectric properties. More detailed studies of the enhancement mechanism will be investigated in the future, as well as a detailed study of the mixed valency with more precise methods.

Overall the figure of merit  $ZT$  of the samarium phase is approximately 40 times larger than that of the yttrium phase taking a value around 0.13 at 1050 K, and extrapolated value of  $\sim 0.4$  at 1500 K, an expected working temperature of topping cycles in thermal power plants. These values are obtained for an initial unmodified compound, and with doping e.g. with transition metals, further improvements are hoped for. Considering that these borides are one of the few really very-high temperature systems for thermoelectrics e.g. for topping cycles in thermal power plants, concentrated solar power and waste heat applications in steelworks, and they do not have precious elements as a main constituent, this work reveals  $\text{SmB}_{62}$  as a promising material to study further.

#### Author Contributions

T.M. and L.S. conceived and designed the study. A.S. grew the  $\text{SmB}_{60}$  crystal and T.T. gave advice on the crystal growth. A.S. cut the crystals and measured the thermoelectric properties and SEM. A.U.K. carried out the Rietveld refinement. T.M. measured the magnetic susceptibility, and made analysis and discussion of all the experimental data. A.S., L.S., and T.M. mainly wrote the manuscript and all authors contributed.

#### References

- [1] Koumoto K, Mori T, editors. Thermoelectric nanomaterials: materials design and applications, vol. 182. Heidelberg: Springer; 2013.
- [2] Zhang X, Zhao LD. Thermoelectric materials: energy conversion between heat and electricity. *J Materiomics* 2015;1:92–105.
- [3] Wood C, Emin D. Conduction mechanism in boron carbide. *Phys Rev B* 1984;29:4582–7.
- [4] Mori T, Berthebaud D, Nishimura T, Nomura A, Shishido T, Nakajima K. Effect of Zn doping on improving crystal quality and thermoelectric properties of borosilicides. *Dalton Trans* 2010;39:1027–30.
- [5] Mori T. Boride thermoelectrics: high temperature thermoelectric materials. In: Rowe DM, editor. Modules, systems, and applications in thermoelectrics. London: CRC Press Taylor and Francis; 2012. p. 14.
- [6] Cahill DG, Fischer HE, Watson SK, Pohl RO, Slack GA. Thermal properties of boron and borides. *Phys Rev B* 1989;40:3254–60.
- [7] Mori T. Thermal conductivity of a rare-earth B12-icosahedral compound. *Phys B Condens Matter* 2006;383:120–1.
- [8] Slack GA. The thermal conductivity of nonmetallic crystals. In: Seitz F, Turnbull D, Ehrenreich H, editors. Solid state physics, vol. 34. New York: Academic Press; 1979. p. 1–71.
- [9] Mori T, Martin J, Nolas G. Thermal conductivity of  $\text{YbB}_{44}\text{Si}_2$ . *J Appl Phys* 2007;102:073510.
- [10] Wang XJ, Mori T, Kuzmych-Ianchuk I, Michiue Y, Yubuta K, Shishido T, et al. Thermal conductivity of layered borides: the effect of building defects on the thermal conductivity of  $\text{TmAlB}_4$  and the anisotropic thermal conductivity of  $\text{AlB}_2$ . *Apl Mater* 2014;2:046113.
- [11] Mott NF. Conduction in glasses containing transition metal ions. *J Non-Cryst Solids* 1968;1:1–17.
- [12] Mori T. Higher borides. In: Gschneidner Jr KA, Bunzli JC, Pecharsky V, editors. Handbook on the physics and chemistry of rare earths, vol. 38. North-Holland: Elsevier BV; 2008. p. 105–73.

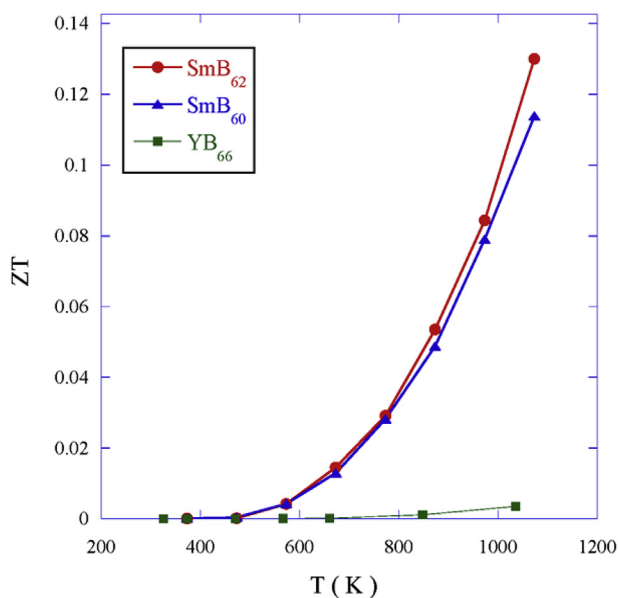


Fig. 11. Temperature dependence of the figure of merits of  $\text{SmB}_{62}$  and  $\text{SmB}_{60}$  crystals compared to  $\text{YB}_{66}$  [25,6].

- [13] Aselage TL, Emin D, McCready SS, Duncan RV. Large enhancement of boron carbides' seebeck coefficients through vibrational softening. *Phys Rev Lett* 1998;81:2316–9.
- [14] Bouchacourt M, Thevenot F. The correlation between the thermoelectric properties and stoichiometry in the boron carbide phase B4C-B10.5C. *J Mater Sci* 1985;20:1237–47.
- [15] Cai KF, Nan CW, Min XM. The influence of silicon dopant and processing on thermoelectric properties of B4C ceramics. *MRS Proc* 1998;545:131.
- [16] Mori T, Nishimura T. Thermoelectric properties of homologous p- and n-type boron-rich borides. *J Solid State Chem* 2006;179:2908–15.
- [17] Mori T, Nishimura T, Yamaura K, Takayama-Muromachi E. High temperature thermoelectric properties of a homologous series of n-type boron icosahedra compounds: a possible counterpart to p-type boron carbide. *J Appl Phys* 2007;101:093714.
- [18] Berthebaud D, Nishimura T, Mori T. Thermoelectric properties and spark plasma sintering of doped YB 22C2N. *J Mat Res* 2010;25:665–9.
- [19] Mori T, Nishimura T, Schnelle W, Burkhardt U, Grin Y. The origin of the n-type behavior in rare earth borocarbide Y1-xB28.5C4. *Dalton Trans* 2014;43:15048.
- [20] Slack GA, Rosolowski JH, Hejna C, Garbaskas M, Kasper JS. Semiconducting properties of boron. In: Werheit H, editor. *Proceeding 9th International Symposium boron, borides and related compounds*. Duisburg: University of Duisburg; 1987. p.132.
- [21] Werheit H, Schmechel R, Kueffel V, Lundström T. On the electronic properties of  $\beta$ -rhombohedral boron interstitially doped with 3d transition metal atoms. *J Alloys Compd* 1997;262–263:372–80.
- [22] Takizawa H, Haze N, Okamoto K, Uheda K, Endo T. Microwave synthesis of Fe-doped  $\beta$ -rhombohedral boron. *Mater Res Bull* 2002;37:113–21.
- [23] Sologub O, Matsushita Y, Mori T. An  $\alpha$ -rhombohedral boron-related compound with sulfur: synthesis, structure and thermoelectric properties. *Scr Mater* 2013;68:289–92.
- [24] Golikova OA, Amandzhanov N, Kazanin MM, Klimashin GM, Kutasov VV. Electrical activity of impurities in  $\beta$ -rhombohedral boron. *Phys Status Solidi A* 1990;121:579–86.
- [25] Mori T, Tanaka T. Effect of transition metal doping and carbon doping on thermoelectric properties of YB66 single crystals. *J Solid State Chem* 2006;179:2889–94.
- [26] Mori T. High temperature thermoelectric properties of B12 icosahedral cluster-containing rare earth boride crystals. *J Appl Phys* 2005;97:093703.
- [27] Berthebaud D, Sato A, Michiue Y, Mori T, Nomura A, Shishido T, et al. Effect of transition element doping on crystal structure of rare earth borosilicides REB44Si2. *J Solid State Chem* 2011;184:1682–7.
- [28] Wan LF, Beckman SP. Lattice instability in the AlMgB14 structure. *Phys B Condens Matter* 2014;438:9–12.
- [29] Miura S, Sasaki H, Takagi K, Fujima T. Effect of varying mixture ratio of raw material powders on the thermoelectric properties of AlMgB14-based materials prepared by spark plasma sintering. *J Phys Chem Solids* 2014;75:951–3.
- [30] Maruyama S, Miyazaki Y, Hayashi K, Kajitani T, Mori T. Excellent p-n control in a high temperature thermoelectric boride. *Appl Phys Lett* 2012;10:152101.
- [31] Maruyama S, Nishimura T, Miyazaki Y, Hayashi K, Kajitani T, Mori T. Microstructure and thermoelectric properties of YxAlyB14 samples fabricated through the spark plasma sintering. *Mater Renew Sustain Energy* 2014;3:31.
- [32] Sahara R, Mori T, Maruyama S, Miyazaki Y, Hayashi K, Kajitani T. Theoretical and experimental investigation of the excellent p-n control in yttrium aluminoborides. *Sci Technol Adv Mater* 2014;15:035012.
- [33] Slack GA, Morgan KE. Some crystallography, chemistry, physics, and thermodynamics of B12O2, B12P2, B12As2, and related alpha-boron type crystals. *J Phys Chem Solids* 2014;75:1054–74.
- [34] Wachter P. Chapter 132 Intermediate valence and heavy fermions. In: Gschneidner Jr KA, Eyring L, Lander GH, Choppin GR, editors. *Handbook on the physics and chemistry of rare earths*, 19; 1994. p. 177–382.
- [35] Nickerson J, White R, Lee K, Bachmann R, Geballe T, Hull G. Physical properties of SmB6. *Phys Rev B* 1971;3:2030–42.
- [36] Gabáni S, Bauer E, Berger S, Flachbart K, Paderno Y, Paul C, et al. Pressure-induced fermi-liquid behavior in the kondo insulator SmB6 : possible transition through a quantum critical point. *Phys Rev B* 2003;67:172406.
- [37] Roman J, Pavlík V, Flachbart K, Herrmannsdörfer T, Rehmann S, Konovalova ES, et al. Transport and magnetic properties of mixed valent SmB6. *Phys B Condens Matter* 1997;230–232:715–7.
- [38] Dzero M, Galitski V. A new exotic state in an old material: a tale of SmB6. *J Exp Theor Phys* 2013;117–3:499–507.
- [39] Lu F, Zhao J, Weng H, Fang Z, Dai X. Correlated topological insulators with mixed valence. *Phys Rev Lett* 2013;110:096401.
- [40] Phelan WA, Koohpayeh SM, Cottingham P, Freeland JW, Leiner JC, Broholm CL, et al. Correlation between bulk thermodynamic measurements and the low-temperature-resistance plateau in SmB6. *Phys Rev X* 2014;4:1–10.
- [41] Xu N, Biswas PK, Dil JH, Dhaka RS, Landolt G, Muff S, et al. Direct observation of the spin texture in SmB6 as evidence of the topological Kondo insulator. *Nat Commun* 2014;5:4566.
- [42] Wolgast S, Kurdak Ç, Sun K, Allen JW, Kim DJ, Fisk Z. Low-temperature surface conduction in the kondo insulator SmB6. *Phys Rev B Condens Matter Mater Phys* 2013;88:1–5.
- [43] Jiang J, Li S, Zhang T, Sun Z, Chen F, Ye ZR, et al. Observation of possible topological in-gap surface states in the kondo insulator SmB6 by photoemission. *Nat Commun* 2013;4:3010.
- [44] Zhu ZH, Nicolaou A, Levy G, Butch NP, Syers P, Wang XF, et al. Polarity-driven surface metallicity in SmB6. *Phys Rev Lett* 2013;111:2–6.
- [45] Takimoto T. SmB6: a promising candidate for a topological insulator. *J Phys Soc Jpn* 2011;80:123710.
- [46] MÜchler L, Yan B, Casper F, Chadov S, Felser C. Topological insulator [Chapter 6]. In: Koumoto K, Mori T, editors. *Thermoelectric nano-materials: materials design and applications*. Heidelberg: Springer; 2013. p. 123–39.
- [47] Paderno YB, Lundström T. On the homogeneity ranges of LaB6, EuB6 and SmB6. *Acta Chem Scand A* 1983;37:609–16.
- [48] Solov'yev GI, Spear KE. Phase behaviour in the Sm-B system. *J Am Ceram Soc* 1972;55–9:475–9.
- [49] Golikova OA, Tadzhev A. Electrical properties of MB66 compounds. *J Less-Common Met* 1981;82:169–71.
- [50] Tanaka T, Rek ZU, Wong J, Rowen M. FZ crystal growth of monochromator-grade YB66 single crystals as guided by topographic and double-crystal diffraction characterization. *J Cryst Growth* 1998;192:141–51.
- [51] Slack GA, Oliver DW, Brower GD, Young JD. Properties of melt-grown single crystal of "YB68". *J Phys Chem Solids* 1977;38:45–9.
- [52] Prytulak A, Mori T. Effect of transition-metal additives on thermoelectric properties of YB22C2N. *J Electron Mater* 2011;40:920–5.
- [53] Prytulak A, Maruyama S, Mori T. Anomalous effect of vanadium boride seeding on thermoelectric properties of YB22C2N. *Mat Res Bull* 2013;48:1972–7.
- [54] Flachbart K, Gabani S, Mori T, Siemensmeyer K. Magnetic ordering in boron-rich borides TbB66 and GdB66. *Acta Phys Pol* 2010;118:875–6.
- [55] Kim H, Bud'ko SL, Tanatar MA, Avdashchenko DV, Matovnikov AV, Mitroshenkov NV, et al. Magnetic properties of RB66 (R = Gd, Tb, Ho, Er, and Lu). *J Supercond Nov Magn* 2012;25:2371–5.
- [56] Novikov VV, Avdashchenko DV, Bud SL. Spin glass and glass-like lattice behaviour in HoB66 at low temperatures. *Philos Mag* 2013;93:1110–23.
- [57] Yazawa K, Koh YR, Shakouri A. Optimization of thermoelectric topping combined steam turbine cycles for energy economy. *Appl Energy* 2013;109:1–9.
- [58] Kajikawa T. The concept of thermoelectric power generation topping-up co-generation system. In: Rowe DM, editor. *Thermoelectrics handbook: macro to nano*. Boca Raton: CRC Press; 2006. 51–1.
- [59] Yazawa K, Hao M, Wu B, Silaen AK, Zhou CQ, Fisher TS, et al. Thermoelectric topping cycles for power plants to eliminate cooling water consumption. *Energ Convers Manage* 2014;84:244–52.
- [60] Liao PK, Spear KE, Schlesinger ME. The B-Sm (Boron-Samarium) system. *J Phase Equilib* 1996;17:347–50.
- [61] Mordovin OA, Timofeeva EN. Rare-earth element hexaborides. *Russ J Inorg Chem* 1968;13:1627–9.



**Mr. Alif Sussardi**, NIMS & Univ. Tsukuba, Tsukuba, Japan. Email: [SUSSARDI.Alifnurpatriya@nims.go.jp](mailto:SUSSARDI.Alifnurpatriya@nims.go.jp). Mr. Alif Sussardi is a Master Course student in the NIMS course at the University of Tsukuba. He did his undergraduate studies in the Bandung Institute of Technology in Indonesia. He is now working on the topic of thermoelectric borides in the Mori Lab.



**Prof. Takao MORI**, NIMS & Univ. Tsukuba, Tsukuba, Japan. Email: [MORI.Takao@nims.go.jp](mailto:MORI.Takao@nims.go.jp). Prof. Takao Mori's present research fields focus on Thermoelectrics, Magnetism, Solid State Physics, Inorganic Materials Science, and Material Synthesis. He is particularly interested in inorganic compounds with “network” structures; atomic clusters, cages, and nets. One particular focus is to develop thermoelectric materials viable for the first wide scale applications. From 2010 Prof. Mori has been a Visiting Professor at Hiroshima University and he is

also Deputy Director at the Center of Materials Research for Low Carbon Emission, and Adj. Prof. at Univ. of Tsukuba. Prof. Mori is also Lab Director of the NIMS Open Innovation Center (NOIC), Thermal Energy Conversion Lab, which is a multi-company and institute open innovation endeavor carrying out challenging research on thermoelectrics and thermal management.



**Prof.em. Louis SCHLAPBACH**, NIMS Tsukuba, Japan. Email: [louis.schlapbach@me.com](mailto:louis.schlapbach@me.com). Dr.sc.nat.ETH Louis Schlapbach was Professor of Experimental Physics at Fribourg University (1987–2000) and ETH Zurich and Director of Empa – a Materials Science and Technology Institution of the ETH Domain (2000–2009). Since 2009 he is frequent guest scientist at NIMS parallel to his work for the Swiss National Science Foundation. His research focused on solid state and surface science with a specialization on materials for energy technologies

(hydrogen). He has published over 300 papers in refereed international journals, some books and book chapters, h-index >50.